Journal Name

ARTICLE

Antiviral Activity of Self-Assembled Glycodendro[60]fullerene Monoadducts

Received 00th January 20xx,
Accepted 00th January 20xx

DOI: 10.1039/x0xx00000x

www.rsc.org/

Antonio Muñoz,[a, b] Beatriz M. Illescas, *[a] Joanna Luczkowiak,[c] Fátima Lasala,[c] Renato Ribeiro-Viana,[d,e] Javier Rojo, *[d] Rafael Delgado*[c] and Nazario Martín*[a,f]

A series of amphiphilic glycodendro[60]fullerene monoadducts were efficiently synthesized using the CuAAC "click chemistry" approach. These glycodendrofullerenes can self-assemble in aqueous media, in a process favoured through π-π interactions between the [60]fullerene moieties. This aggregation process leads to big and well-defined compact micelles with a uniform size and spherical-shape. The supramolecular aggregate was characterized using electronic microscopy (SEM and TEM), light scattering methods (DLS) and X-ray methodologies (SAXS and XRD). The antiviral efficiency of these aggregates has been tested in an experimental infection assay using Ebola virus glycoprotein (EboGP) pseudotyped viral particles on Jurkat cells overexpressing DC-SIGN and it is observed an improvement of the IC_{50} value with respect to other systems endowed with a higher number of carbohydrate ligands.

1. Introduction

Nowadays, new disciplines such as glycobiology and glycochemistry have an increasing interest.[1, 2] The total synthesis of glycoforms that are present in the glycome of living beings is currently a great challenge for organic chemistry. The chemical sciences have alternative tools to the complex total synthesis of these natural glycoforms. An interesting option is the design of artificial glycomimetics which mimic the glycosylated surface of many pathogens, such as virus, bacteria or protozoos. The chemical modification and a rational design of these new glycomolecules allow obtaining a strong multivalent interaction.[3, 4] This interaction occurs through two forms of recognition, sugar-protein and sugar-sugar, implicated in many vital bioprocesses such as pathogen recognition, celullar differentiation, adhesion of infectious pathogens to host cells and other processes in which glycoma is directly involved.[5, 6] The new glycomimetics and their spatial topographical presentation is associated with the ''glycocode'', which provides the fundamental tools for specific and high affinity ''lock-in'' multivalent recognition events.

Hence, multivalent effect is essentially generated by properly oriented architectures on the cell surface which provide a strategy for controlling signal transduction pathways through interaction with these well-oriented cellular receptors, triggering a specific biological process.[7] In order to design multivalent peripheral ligands with glycomimetic properties that structurally can attach to the receptor sites of complex biological structures, a broad variety of ''artificial glycoforms'' have been created to study and understand the mechanisms involved in multivalent binding interactions.[8, 9] The mechanisms by which this was found to be operational include receptor clustering on the cell surface, chelation, steric stabilization, subsite-assisted binding, and statistical rebinding phenomena.[10] Some of these mechanisms seem to be favored by a spherical scaffold which will result in a globular symmetry in the glycomimetic structure. This point was demonstrated when hexakis-adducts of [60]fullerene decorated with carbohydrates ("Fullerene Sugar Balls") were synthesized.[11] This special class of molecules, based on a C_{60} scaffold, allows obtaining a

[a] Departamento de Química Orgánica, Fac. C.C. Químicas, Universidad Complutense de Madrid, Av. Complutense s/n, 28040 Madrid (Spain).
[b] School of Chemistry, Yachay Tech University, Yachay City of Knowledge, 100115, Urcuqui (Ecuador).
[c] Laboratorio de Microbiología Molecular Instituto de Investigación Hospital 12 de Octubre (imas12), 28041 Madrid, Spain.
[d] Glycosystems Laboratory Instituto de Investigaciones Químicas (IIQ) CSIC – Universidad de Sevilla Av. Américo Vespucio 49, 41092 Seville, Spain.
[e] Present address: Departamento Academico de Química, Universidade Tecnologica Federal do Paraná. Av dos Pioneiros, 3131. Londrina - PR - Brazil.
[f] Instituto Madrileño de Estudios Avanzados en Nanociencia (IMDEA-Nanociencia), Campus UAM, Cantoblanco, E-28049, Madrid, Spain.

Electronic Supplementary Information (ESI) available: Synthesis and characterization of 1a-b and 2a-, SEM and TEM images, DLS experiments and biological assays. See DOI: 10.1039/x0xx00000x

monodisperse molecule with a spherical shape in a straightforward manner.[12] These molecules showed their biological multivalent activity in dynamics NMR experiments,[13] isothermal titration calorimetry[12] and inhibition of viral infection studies *in vitro* with human cells.[14, 15] From the work carried out by our group on glycofullerenes with globular symmetry, it is possible to bring to light the significance of size and shape of the glycomimetic, being even more determinant that the number of carbohydrate moieties in the glycoparticle**.**

In the present work, we have tried to reach adequate size and geometry, for the multivalent presentation of carbohydrate moieties using supramolecular chemistry. The supramolecular approach allows a significant synthetic simplification, and avoids the handling of polydispersed polymers or macromolecular structures, through the self-assembly of well characterized amphiphilic molecules. In a previous work, we studied the self-assembly properties of several amphiphilic dendrofullerenes in aqueous media, obtaining different supramolecular arrangements, from nanorods to nanovesicles.[16] The molecules prepared in this work should, in principle, have a similar behaviour in aqueous media as they present the same amphiphilic nature, sharing also the C_{60} units, responsible of the creation of π-π staking interactions that lead to supramolecular aggregates. In the present work, the synthetic approach is simplified, using C_{60} mono-adducts instead of C_{60} hexakis-adducts, without compromising the spherical form of the final glycomimetic, provided by the supramolecular aggregate resulting from the self-assembly of mono-adducts.

DC-SIGN (Dendritic Cell-Specific Intercellular adhesion molecule-3-Grabbing Non-integrin) is a C-type lectine present on the surface of inmatured dendritic cells. DC-SIGN is considered as a universal receptor for pathogens in the human immune system.[17] It recognizes some glycosylated surfaces, specially mannosylated and fucosylated glycans in a Ca^{2+} dependent multivalent way and this recognition process is the initial stage for infection by some viruses, like Dengue, HIV and Ebola.[18] Mannose units presented in a multivalent manner can be used as a glycomimic of natural Ebola Virus in its interaction with DC-SIGN, while glycodendrons containing galactose will be used as a negative control, as they do not interact with DC-SIGN.

We have synthesized a short series of glycodendrons which have a pending C_{60} unit. The self-assembly of these derivatives yields spherical aggregates of micelle type that show improved biological activity in the inhibition of viral infection in a synthetic Ebola virus experimental model.

2. Results and discussion

2.1. Synthesis and Characterization

To synthesize the new glycodendrofullerenes **1a-b** and **2a-b** (Fig. 1) we have employed an efficient click chemistry strategy.[19, 20] Thus, we have carried out the Cu(I)-catalyzed azide-alkyne 1,3-dipolar cycloaddition reaction (CuAAC)[21] between the fullerene properly modified with terminal alkyne moieties[16] and mannose or galactose glycodendrons endowed with an azide group in their focal position.[22] The CuAAC reaction was carried out in the presence of metallic copper, $CuBr{\cdot}SMe_2$ as source of Cu (I) and DMSO as solvent, following the optimized methodology previously reported. This methodology allows obtaining high yields and minimizing the chromatographic processes (See SI).

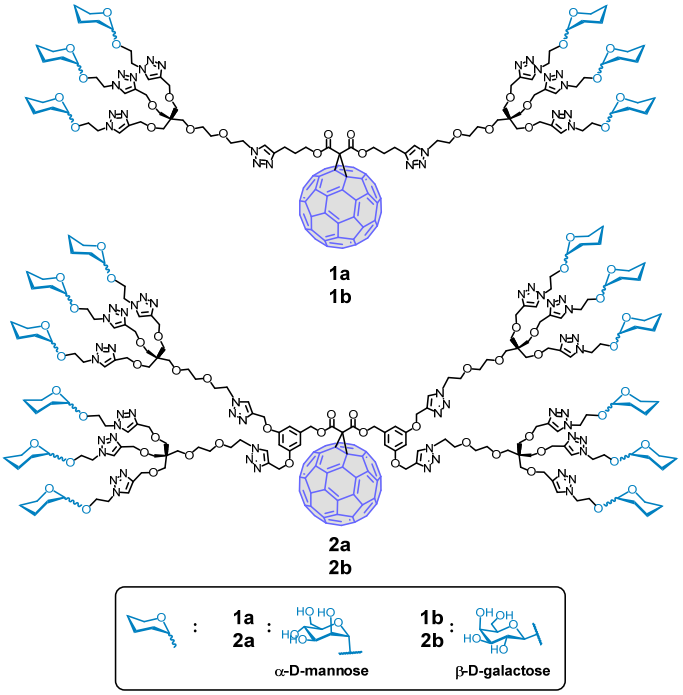

Fig. 1 Chemical structure of synthesized glycofullerenes **1a-b** and **2a-b**.

Characterization of the products was carried out by standard spectroscopic and analytical techniques. Thus, completion of the click reaction can be easily confirmed by the presence of the characteristic signals for the protons of the 1,2,3-triazole rings, which appear as a broad singlet around 7.8 ppm in the ^{1}H NMR spectra. In the ^{13}C NMR spectra, four signals (at δ ~ 146, 144, 124 and 123) are observed for the two different types of triazole rings present in each derivative. Also, the disappearance of the alkyne and azide signals in the IR spectra (~ 2100 and 2090 cm^{-1} respectively) was a clear evidence of the complete functionalization via CuAAC reaction of the alkyne fullerene derivatives.

Mass spectrometry studies corroborate the molecular mass expected for compounds **1a-b** and **2a-b**. MALDI-TOF mass spectra show a broad distribution of masses, centred on the calculated *m/z* molecular peak, as usually observed for glycodendrimeric structures described in the bibliography (See SI).[23, 24]

During the spectroscopic characterization, first evidences of supramolecular aggregation were observed. ^{13}C-NMR spectra reveal the lack of the 15 signals corresponding to the sp^2 carbons of the C_{60} unit, which typically appear between 139 and 147 ppm, despite the high solubility in water and other polar solvents of these glycodendrofullerenes (~15 mg/mL in water and ~25 mg/mL in DMSO for **1a** and **2a,** respectively). Increasing the concentration or diluting the samples did not show the signals belonging to the C_{60} scaffold in ^{13}C NMR experiments. This behaviour suggests strong π-π interactions between C_{60} units, promoted probably by solvophobic effects due to the surrounding polar media which avoid the contact between the deuterated solvent and the C_{60} fragment in the molecules.[25] Therefore, the possible formation of a supramolecular aggregate is foreseen, more likely of spherical shape, like vesicles or micelles. In order to confirm this supposition, we carried out aggregation studies using different techniques.

Scanning electron microscopy (SEM) images of a solution of glycodendrofullerenes (1 μM) in water on a glass substrate showed clearly the formation of giant spherical aggregates of similar and uniform size for glycofullerenes which contain 6 (**1a-b**) and 12 (**2a-b**)

carbohydrate moieties. These aggregates reach sizes of around 60 µm, an unusual big size for self-assembled fullerene-based structures in aqueous media (Figs. 2 and S1).[26, 27] TEM images obtained from freshly prepared 1 µM water solutions deposited on carbon-coated grids show the formation of micelles with diameters varying from 100-170 nm (Fig. S4, SI).

Dynamic Light Scattering (DLS) measurements confirmed the coexistence of these spherical aggregates with free glycodendrofullerene molecules in water. The biggest aggregates can be removed by filtration, but the solvophobic interactions start again the formation of these aggregates until the equilibrium state is reached and the coexistence of individual molecules and spherical aggregates of ~100 nm and ~60 µM is observed. This aggregation process can be monitored through DLS measurements, comparing freshly filtered solutions of glycodendrofullerenes, and their evolution along a period of 5 hours at room temperature (Figs. S2 and S3, SI).

XRD and low angle X-ray scattering (SAXS) experiments were performed in order to elucidate the internal structure and glycodendrofullerene´s organization level within the supramolecular micellar aggregate. XRD experiments were carried out in powder for compounds **1a** and **2**a. Diffractograms showed a clear diffraction pattern identical for both fullerene derivatives with only one diffraction maximum at 2θ = 8.3, corresponding to a spacing of 1 nm. This spacing is assigned to the packing between the C_{60} subunits of the glycofullerenes, with uniform arrangement within the micelle.

In order to determine higher spacing arrangements, SAXS experiments in aqueous solutions of glycofullerenes **1a** and **2a** were performed, where two clear diffractions corresponding to the parameter q_1= 0.091 Å $^{-1}$ and q_2= 0.6 Å $^{-1}$ were observed. The spacing (d=2π/q) for q_1 is 7 nm, and is equivalent to the smaller micelle repeated pattern in its radial axis, corresponding to two glycofullerene molecules faced by their C_{60} subunits. The spacing corresponding to q_2 is the same observed in XRD, that is, 1 nm, corresponding to the C_{60}-C_{60} packaging within the micellar structure. This compact packaging suggests that the C_{60} subunits are poorly solvated, which would explain the absence of the typical ^{13}C NMR signals for the C_{60} moiety in Bingel-type mono-adducts.[28] In the SAXS measurements no other diffractions were observed indicating a higher order in the arrangement within the supramolecular aggregate, which indicates that the formed aggregates appear to be solid collapsed multilamellar micelles.[29, 30]

The experimental results obtained by SAXS are in agreement with the observations in SEM images, where some partially broken micelles are observed, revealing their clearly solid and compact inner part. All experimental data show practically identical results for the glycofullerenes containing 6 or 12 carbohydrates, indicating that both systems behave in the same way when self-assembling, suggesting that the C_{60} subunit manages the packaging and is a key part in the formation of these supramolecular aggregates. It is expected that the self-assembled structures of the molecule **2a** (with 12 carbohydrate units), possess a surface with greater density of carbohydrates, because the packing between the C_{60} units presented the same pattern in both molecular systems.

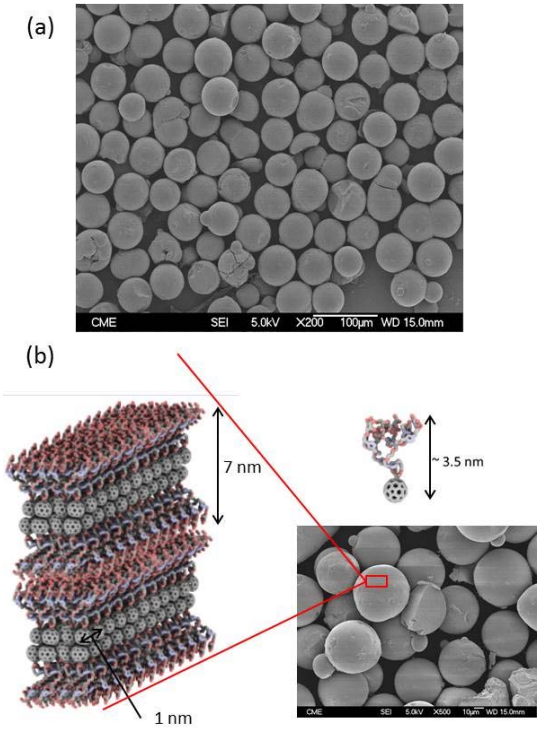

Fig. 2 (a) SEM micrograph of **1a** obtained by deposition of a 1 µM water solution on a glass substrate. Abundant aggregates of 50-60 µm are observed. (b) Amplified micrograph where the compact internal structure of the micelles is showed. Cartoon showing the packing of the molecules in the micelles.

2.2. Biological Studies

DC-SIGN is a C-type lectin receptor present on the surface of both macrophages and dendritic cells. It has been proposed as receptor for the entry of Ebola virus (EBOV) and HIV.[18, 31, 32]

Although DC-SIGN is not the only receptor for EBOV, it is thought to play a significant role as a gate for cell entry of this infectious agent in the first stages of the infection process.[18] DC-SIGN targeting is a good strategy for studying the first steps of infection processes of EBOV. DC-SIGN is able to recognize mannosylated and fucosylated residues presented in a multivalent way on the surface of several pathogens. Therefore, the new artificial multivalent systems, obtained through a supramolecular self-assembly, can compete with the natural ligands present in viruses and other pathogens for the same cellular receptors. In this study we have evaluated the inhibitory effect of self-assembled glycofullerenes in an experiment of the direct infection of Jurkat cells that over-express the receptor DC-SIGN on their surface (DC-SIGN$^+$ Jurkat) using pseudotyped viral particles that present an envelope of EBOV-GP. These self-assembled and globular multivalent systems are water soluble, which allow the study of their potential biological function in blocking viral infection.

The results of inhibition studies of the DC-SIGN receptor by different compounds are reported as a function of concentration (Fig. 3). The IC_{50} inhibition of the infection was obtained with a 95% confidence interval. Galactose-containing molecules **1b** and **2b** were used as negative controls, because the galactose moieties are not recognized by DC-SIGN. As additional control, infection with DC-SIGN-independent vesicular stomatitis virus envelope GP (VSV-GP)-pseudotyped lentiviral particles was performed under the same conditions.[33] For compound **1a**, which contains 6 mannose units, an IC_{50} of 424 nM was obtained, and for compound **2a** which contains 12 units

of mannose, the IC_{50} was 196 nM. Previous results using hexakis-adducts of [60]fullerene endowed with 12 mannose moieties[15] show relative inhibitory potency (RIP) values one order of magnitude smaller (Table 1). Compound **1a** and **2a** were also tested for cytotoxicity in a proliferation assay (Fig. 4). Compound **2a** showed some effect on cell metabolism at doses 10^3 nM and above that is lower than the effect on the infection with the EBOV-GP pseudotyped construction and it was not evident with the VSV-G pseudotyped control. No cell toxicity was experienced with compound **1a**. So, we think that the infection inhibition observed is reasonably DC-SIGN blockage dependent. Therefore, these results demonstrate that self-assembly amplifies DC-SIGN blockade and enhances antiviral activity (Fig. S7), when it is compared to multivalent globular systems containing similar or greater number of carbohydrate moieties per molecule. The self-assembly of the molecules leads to micellar structures of globular symmetry comparable in size to that of a virus or other bacterial pathogens.

Table 1. Comparative of IC_{50} values and relative inhibitory potency (RIP) of glycodendrofullerenes **1a** and **2a** with fullerene hexakis-adduct with 12 mannose moieties C60(12Man) in inhibition studies using pseudotyped Ebola virus particles.

Compound	IC_{50} (nM)	n Mannoses	RIP[a]
C60(12Man)[15]	2000	12	53
1a	424	6	500
2a	196	12	540
α-Methyl Man[b, 34]	$1.27x10^6$	1	1

[a] Relative inhibitory potency (RIP), calculated as (IC_{50})mono/$(IC_{50}$*valency); [b] α-methyl-D-mannopyranoside

Conclusions

One of the main problems found in the inhibition of DC-SIGN with a multivalent artificial glycomimic, is the construction of systems with an adequate size and multivalency to mimic natural systems such as viruses. In this work it is shown that by simple chemical synthesis, monoadducts of spherical [60]fullerene capable of self-assembling can be obtained to form a supramolecular aggregate of micellar nature, with a surface with high carbohydrate density and satisfactory size and shape. A thorough study of the new fullerene derivatives has been carried out by spectroscopic and analytical means, whereas a variety of techniques, namely electronic microscopy (SEM and TEM), light scattering methods (DLS) and X-ray methodologies (SAXS and XRD) have been used for the supramolecular characterization. Remarkably, this supramolecular association significantly improves biological properties and is able to inhibit DC-SIGN in the range of nanomolarity.

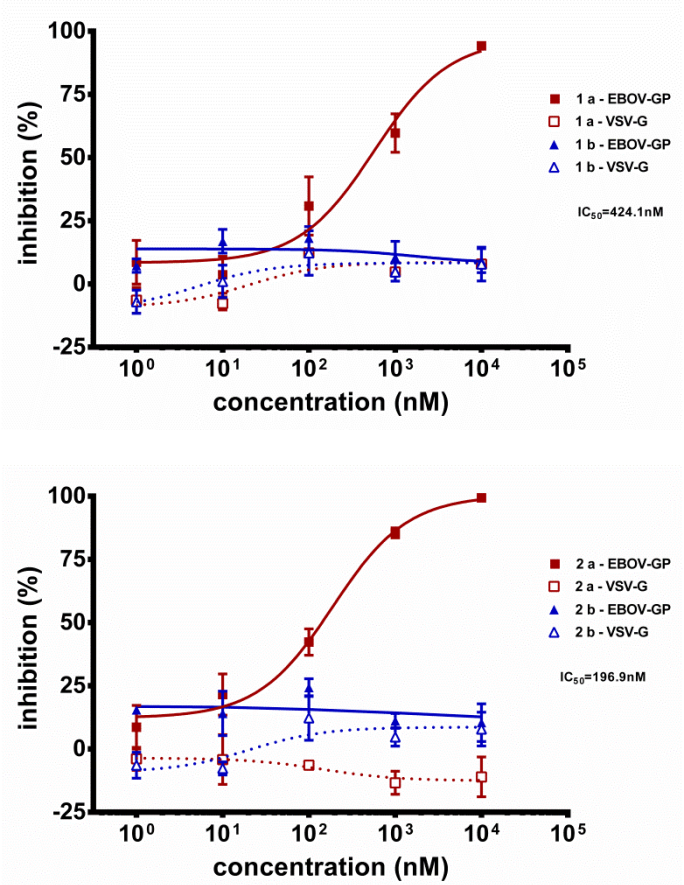

Fig. 3. a) Inhibition of infection with EBOV or VSV GP-pseudotyped lentiviral particles of Jurkat DC-SIGN+ cells using **1a** (red) and **1b** (blue). In the cis-infection experiments $2.5x10^5$ Jurkat DC-SIGN+ were challenged with 5000 TCID of recombinant lentiparticles. b) Inhibition of infection with EBOV or VSV GP-pseudotyped lentiviral particles of Jurkat DC-SIGN+ cells using **2a** (red) and **2b** (blue). In the cis-infection experiments $2.5x10^5$Jurkat DC-SIGN+ were challenged with 5000 TCID of recombinant lentiparticles. In both cases, results represent mean of 3 independent experiments +/- SEM.

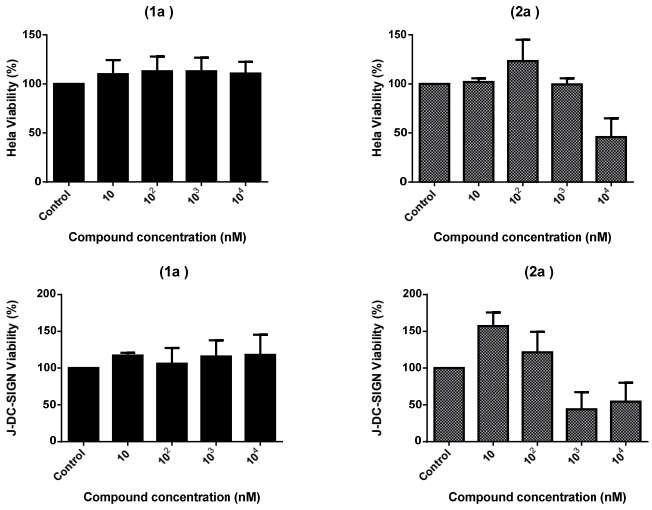

Fig. 4. Cell proliferation assay using glycofullerenes **1a** and **2a**.

Experimental Section

General.-Compounds **3**,[16] **4**[16] and **5a-b**[22] were prepared according to previously reported procedures. All reactions were performed in standard glassware under an inert Ar or N_2 atmosphere. Column chromatography: silica gel 60 (230-400 mesh, 0.040-0.063 mm) was purchased from E. Merck. Thin Layer Chromatography (TLC) was performed on glass sheets coated with silica gel 60 F254 purchased from E. Merck, visualization by UV light. IR spectra (cm-1) were measured on an BRUKER ALPHA- FTIR instrument with ATR. NMR spectra were recorded on a Bruker AVIII 700MHz, AV. 500 or DPX 300MHz with solvent peaks as reference. MALDI-TOF-mass spectra were carried out on a Bruker ULTRAFLEX matrix assisted laser desorption time-of-flight mass spectrometer. Dynamic Light Scattering measurements were carried out on an ALV GSC08 correlator working in a cross correlation mode with an Ar^+ laser operating at λ = 514.5 nm. The output signals were obtained with backscatter detection at an angle of 30° and processed with a digital correlator that computed intensity-intensity autocorrelation of the scattered light. Measurements were made in a 1-cm path-length round quartz cell maintained at 298 K. Solution samples were filtered through nylon Acrodisc syringe filters (Pall Life Sciences) with 0.2-µm pore size. SEM images were obtained from on a JEOL JSM 6335F microscope working at 5kV or 10kV. TEM measurements were performed on a JEOL JEM 2100 electron microscope, operating at an acceleration voltage of 200 kV. SAXS experiments were obtained from PANalytical PW3830 X-Ray generator using a Kratky Chamber modified by Hecus-Braun.

Synthesis of glycodendrofullerenes 1a-b and 2a-b.

General Procedure.- A round bottom vial provided with a magnetic stirrer containing compound alkynyl derivative **3** or **4** (7.2 mg, $7.5{\cdot}10^{-3}$ mmol), glycodendron **5a** or **5b** (1.3 eqs per alkyne moiety), $CuBr{\cdot}S(CH_3)_2$ (6 mg, 0.03 mmol) and sodium ascorbate (13 mg, 0.07 mmol) in the presence of metallic copper wire, was deoxygenated using an argon stream, and then 2 mL of DMSO were added and deoxygenation continued for 3 minutes with vigorous stirring. After that, the reaction mixture was maintained for 48 h with stirring and under an argon atmosphere. After this time, the crude was dissolved in DMSO and passed through a column of functionalized silica gel (QuadraSil Mercaptopropil™). The resulting dark brown solution was precipitated with acetonitrile and centrifuged for 10 min at 4500 rpm. The precipitate was washed and resuspended using AcOEt in an ultrasonic bath for 2 min, then centrifuged for 10 min at 6000 rpm. Compounds **1a-b** and **2a-b** were obtained as bright dark brown solids.

Compound 1a

Yield: 92%; IR-FT (KBr): 3311, 2879, 1739, 1627, 1418, 1354, 1223, 1131, 1094, 1061, 878, 775, 520, 485 cm^{-1}; ^1H NMR (700 MHz, DMSO-d^6), δ: 8.02 (s, 6H), 7.82 (s, 2H), 6.12 (s, 4H), 5.81 (s, 4H), 4.75 (d, J = 4.1, 10H), 4.63 (s, 6H), 4.61–4.55 (m, 12H), 4.52 (m, 6H), 4.50–4.40 (m, 22H), 3.94 (t, J = 4.8, 12H), 3.91–3.86 (m, 9H), 3.82–3.75 (m, 18H), 3.65–3.59 (m, 6H), 3.54 (s, 6H), 3.51 (m, 6H), 3.25 (s, 6H), 3.19–3.14 (m, 12H), 2.53 (m, 9H); ^{13}C NMR(175 MHz, DMSO-d^6), δ: 163.0, 162.7, 146.2, 144.3, 124.5, 123.1, 102.1, 100.3, 80.9, 76.0, 74.5, 73.1, 71.3, 70.5, 69.5, 69.0, 67.2, 65.3, 64.6, 63.7, 61.4, 60.3, 55.5, 49.7, 45.6, 36.1, 31.2, 28.0, 21.8, 21.0, 14.8.; MS (MALDI-TOF) calculated for: $[M]^+$ $C_{157}H_{154}N_{24}O_{50}$ = 3175.02; found: 3199.6 $[M+Na]^+$, 3239.9 $[M+Cu]^+$.

Compound 1b

IR-FT (KBr): 3323, 2888, 1742, 1619, 1592, 1418, 1350, 1217, 1100, 1061, 878, 775, 510 cm^{-1}; ^1H NMR (300 MHz, DMSO-d^6), δ: 8.03 (s, 6H), 7.83 (s, 2H), 5.12 (m, ~4H), 5.01 (s, 4H), 4.75 (m, ~10H), 4.63 (s, ~6H), 4.61–4.55 (m, ~12H), 4.52 (m, 6H), 4.50–4.40 (m, 22H), 3.94–3.92 (m, ~12H), 3.91–3.86 (m, ~9H), 3.82–3.75 (m, ~18H), 3.65–3.59 (m, ~6H), 3.54 (m, ~6H), 3.51 (m, 6H), 3.21 (s, 6H), 3.19–3.11 (m, ~12H), 2.45 (m, ~9H); ^{13}C NMR (175 MHz, DMSO-d^6), δ: 164.2, 163.6, 145.1, 143.1, 125.5, 123.5, 100.7, 99.4, 80.3, 77.7, 74.9, 73.8, 72.96, 70.6, 69.8, 67.0, 65.8, 65.3, 63.26, 61.6, 60.7, 54.2, 48.8, 45.9, 43.1, 35.9, 33.9, 31.1, 30.3, 20.6, 14.1, 13.2; MS (MALDI-TOF) calculated for: $[M]^+$ $C_{157}H_{154}N_{24}O_{50}$ = 3175.02; found: 3175.2.

Compound 2a

IR-FT (KBr): 3321, 2869.0, 1728, 1624, 1422, 1223, 1131, 1091, 881, 520 cm^{-1}; ^1H NMR (700 MHz, DMSO-d^6), δ: 8.03 (s, 2H), 7.87 (s, 6H), 6.58 – 6.51 (m, 4H), 6.47 – 6.41 (m, 2H), 5.00 (s, 4H), 4.74 (d, J = 3.1, ~18H), 4.58 (s, ~16H), 4.24 – 4.13 (m,~ 24H), 4.05 (t, J = 7.9, ~18H), 3.99 –3.93 (m, 12H), 3.91 (m, ~12H), 3.79–3.66 (m, ~8H), 3.63–3.56 (m, ~38H), 3.21–3.06 (m, ~24H), 2.99 (m, ~22H); ^{13}C NMR (175 MHz, DMSO-d^6), δ: 176.2, 165.9, 164.9, 163.4, 159.4, 144.32, 142.8, 126.3, 125.6, 124.9, 118.3, 114.6, 99.6, 73.1, 72.7, 71.3, 70.6, 69.5, 68.7, 66.5, 65.2, 63.9, 63.6, 62.9, 60.6, 52.2, 49.6, 44.9; MS (MALDI-TOF) calculated for $[M]^+$ $C_{253}H_{294}N_{48}O_{100}$= 5603.94; found: 5603.

Compound 2b

IR-FT (KBr): 3326, 2871, 1728, 1624, 1422, 1223, 1203, 1131, 1089, 881, 729, 524 cm^{-1}; ^1H NMR (700 MHz, DMSO-d^6), δ: 8.03(s, 2H), 7.87(s, 6H), 6.55–6.49 (m, 4H), 6.43–6.41 (m, 2H), 5.00 (s, 4H), 4.73(m, ~18H) 4.58(s, ~16H), 4.39–4.17 (m, ~24H), 4.05 (t, J = 7.9, ~18H), 3.98 (m, 12H) 3.88 (m, ~12H), 3.75–3.67 (m, ~8H), 3.58–3.54 (m, ~38H), 3.23–3.04 (m, ~24H), 3.01(m, ~22H); ^{13}C NMR (175 MHz, DMSO-d^6), δ: 177.0, 176.5, 166.4, 165.2, 163.38, 158.9, 144.4, 142.5, 125.5, 125.0, 124.6, 117.5, 99.9, 94.3, 73.1, 72.6, 71.7, 70.5, 70.0, 69.3, 68.2, 66.5, 65.1, 63.9, 62.9, 60.9, 52.6, 51.9, 49.9, 45.1; MS (MALDI-TOF) calculated for $[M]^+$ $C_{253}H_{294}N_{48}O_{100}$= 5603.94; found: 5604.

Acknowledgements

Financial support by the European Research Council (ERC-2012-ADG_20120216 (Chir*all*carbon), ITN-2008-213592 (CARMUSYS)), Ministerio de Economía y Competitividad (MINECO) of Spain (projects CTQ2014-52045-R and CTQ2014-52328-P), the Comunidad Autónoma de Madrid (PHOTOCARBON project S2013/MIT-2841) and Instituto de Salud Carlos III (ISCIII) (FIS1400708 and DTS1500171) is acknowledged.

Notes and references

1. B. Imperiali, *J. Am. Chem. Soc.*, 2012, **134**, 17835-17839.
2. P. H. Seeberger, *Nat. Chem. Biol.*, 2009, **5**, 368-372.
3. M. Mammen, S.-K. Choi and G. M. Whitesides, *Angew. Chem. Int. Ed.*, 1998, **37**, 2754-2794.
4. A. Bernardi, J. Jimenez-Barbero, A. Casnati, C. De Castro, T. Darbre, F. Fieschi, J. Finne, H. Funken, K.-E. Jaeger, M. Lahmann, T. K. Lindhorst, M. Marradi, P. Messner, A. Molinaro, P. V. Murphy, C. Nativi, S. Oscarson, S. Penades, F. Peri, R. J. Pieters, O. Renaudet, J.-L. Reymond, B. Richichi, J. Rojo, F. Sansone, C. Schaffer, W. B. Turnbull, T. Velasco-Torrijos, S. Vidal, S. Vincent, T. Wennekes, H. Zuilhof and A. Imberty, *Chem. Soc. Rev.*, 2013, **42**, 4709-4727.
5. A. Varki, *Glycobiology*, 1993, **3**, 97-130.
6. C. R. Bertozzi, Kiessling and L. L., *Science*, 2001, **291**, 2357-2364.
7. S. Bhatia, L. C. Camacho and R. Haag, *J. Am. Chem. Soc.*, 2016, **138**, 8654-8666.
8. A. Imberty, Y. M. Chabre and R. Roy, *Chem. Eur. J.*, 2008, **14**, 7490-7499.
9. S. Cecioni, A. Imberty and S. Vidal, *Chem. Rev.*, 2015, **115**, 525-561.
10. C. Fasting, C. A. Schalley, M. Weber, O. Seitz, S. Hecht, B. Koksch, J. Dernedde, C. Graf, E. W. Knapp and R. Haag, *Angew. Chem. Int. Ed. Engl.*, 2012, **51**, 10472-10498.
11. J.-F. Nierengarten, J. Iehl, V. Oerthel, M. Holler, B. M. Illescas, A. Munoz, N. Martin, J. Rojo, M. Sanchez-Navarro, S. Cecioni, S. Vidal, K. Buffet, M. Durka and S. P. Vincent, *Chem. Commun.*, 2010, **46**, 3860-3862.
12. M. Sanchez-Navarro, A. Munoz, B. M. Illescas, J. Rojo and N. Martin, *Chem. Eur. J.*, 2011, **17**, 766-769.
13. O. Engstrom, A. Munoz, B. M. Illescas, N. Martin, R. Ribeiro-Viana, J. Rojo and G. Widmalm, *Org. Biomol. Chem.*, 2015, **13**, 8750-8755.
14. A. Muñoz, D. Sigwalt, B. M. Illescas, J. Luczkowiak, L. Rodríguez-Pérez, I. Nierengarten, M. Holler, J.-S. Remy, K. Buffet, S. P. Vincent, J. Rojo, R. Delgado, J.-F. Nierengarten and N. Martín, *Nat. Chem.*, 2016, **8**, 50-57.
15. J. Luczkowiak, A. Muñoz, M. Sánchez-Navarro, R. Ribeiro-Viana, A. Ginieis, B. M. Illescas, N. Martín, R. Delgado and J. Rojo, *Biomacromolecules*, 2013, **14**, 431-437.
16. A. Muñoz, B. M. Illescas, M. Sánchez-Navarro, J. Rojo and N. Martín, *J. Am. Chem. Soc.*, 2011, **133**, 16758-16761.
17. Y. Guo, H. Feinberg, E. Conroy, D. A. Mitchell, R. Alvarez, O. Blixt, M. E. Taylor, W. I. Weis and K. Drickamer, *Nat. Struct. Mol. Biol.*, 2004, **11**, 591-598.
18. C. P. Alvarez, F. Lasala, J. Carrillo, O. Muñiz, A. L. Corbí and R. Delgado, *J. Virol.*, 2002, **76**, 6841-6844.
19. I. Nierengarten and J. F. Nierengarten, *Chem. Rec.*, 2015, **15**, 31-51.
20. H. C. Kolb, M. G. Finn and K. B. Sharpless, *Angew. Chem. Int. Ed.*, 2001, **40**, 2004-2021.
21. R. Huisgen, *Angew. Chem. Int. Ed.*, 1968, **7**, 321-328.
22. R. Ribeiro-Viana, M. Sánchez-Navarro, J. Luczkowiak, J. R. Koeppe, R. Delgado, J. Rojo and B. G. Davis, *Nat. Commun.*, 2012, **3**, 1303.
23. D. J. Harvey, *Mass Spectrom. Rev.*, 2009, **28**, 273-361.
24. M. Durka, K. Buffet, J. Iehl, M. Holler, J.-F. Nierengarten and S. P. Vincent, *Chem. Eur. J.*, 2012, **18**, 641-651.
25. G. M. Soliman, J. Szychowski, S. Hanessian and F. M. Winnik, *Soft Matter*, 2010, **6**, 4504-4514.
26. H. Kato, C. Böttcher and A. Hirsch, *Eur. J. Org. Chem.*, 2007, **2007**, 2659-2666.
27. Y. Zhao and G. Chen, in *Fullerenes and Other Carbon-Rich Nanostructures*, ed. J.-F. Nierengarten, Springer Berlin Heidelberg, Berlin, Heidelberg, 2014, DOI: 10.1007/430_2013_130, pp. 23-53.
28. Z. Lin, P. Lu, C. H. Hsu, K. Yue, X. H. Dong, H. Liu, K. Guo, C. Wesdemiotis, W. B. Zhang, X. Yu and S. Z. Cheng, *Chem. Eur. J.*, 2014, **20**, 11630-11635.
29. Y.-b. Lim and M. Lee, *Org. Biomol. Chem.*, 2007, **5**, 401-405.
30. E. Busseron, Y. Ruff, E. Moulin and N. Giuseppone, *Nanoscale*, 2013, **5**, 7098-7140.
31. A. S. Kondratowicz, N. J. Lennemann, P. L. Sinn, R. A. Davey, C. L. Hunt, S. Moller-Tank, D. K. Meyerholz, P. Rennert, R. F. Mullins, M. Brindley, L. M. Sandersfeld, K. Quinn, M. Weller, P. B. McCray, Jr., J. Chiorini and W. Maury, *Proc. Natl. Acad. Sci. U. S. A.*, 2011, **108**, 8426-8431.
32. J. E. Carette, M. Raaben, A. C. Wong, A. S. Herbert, G. Obernosterer, N. Mulherkar, A. I. Kuehne, P. J. Kranzusch, A. M. Griffin, G. Ruthel, P. Dal Cin, J. M. Dye, S. P. Whelan, K. Chandran and T. R. Brummelkamp, *Nature*, 2011, **477**, 340-343.
33. Z.-y. Yang, R. Delgado, L. Xu, R. F. Todd, E. G. Nabel, A. Sanchez and G. J. Nabel, *Science*, 1998, **279**, 1034-1037.
34. F. Lasala, E. Arce, J. R. Otero, J. Rojo and R. Delgado, *Antimicrob. Agents Chemother.*, 2003, **47**, 3970-3972.